

Tunable many-body burst in isolated quantum systems

Shozo Yamada,^{1,*} Akihiro Hokkyo,^{1,†} and Masahito Ueda^{1,2,3,‡}

¹*Department of Physics, University of Tokyo, 7-3-1 Hongo, Bunkyo-ku, Tokyo 113-0033, Japan*

²*RIKEN Center for Emergent Matter Science (CEMS), Wako, Saitama 351-0198, Japan*

³*Institute for Physics of Intelligence, University of Tokyo,
7-3-1 Hongo, Bunkyo-ku, Tokyo 113-0033, Japan*

Thermalization in isolated quantum many-body systems can be nonmonotonic, with its process dependent on an initial state. We propose a numerical method to construct a low-entangled initial state that creates a “burst”—a transient deviation of an observable from its thermal equilibrium value—at a designated time. We apply this method to demonstrate that a burst of magnetization can be realized for a nonintegrable mixed-field Ising chain on a timescale comparable to the onset of quantum scrambling. Contrary to the typical spreading of information in this regime, the created burst is accompanied by a slow or even negative entanglement growth. Analytically, we show that a burst becomes probabilistically rare after a long time. Our results suggest that a nonequilibrium state is maintained for an appropriately chosen initial state until scrambling becomes dominant. These predictions can be tested with programmable quantum simulators.

Introduction—Ever since von Neumann’s seminal work [1], how irreversible macroscopic thermalization emerges from reversible microscopic laws of quantum mechanics has been actively debated. This fundamental problem of quantum thermalization has attracted wide interest [2–6] due in large part to experimental advances in ultracold atoms [7–14], trapped ions [15–18], and superconducting qubits [19–24]. To resolve this issue, the eigenstate thermalization hypothesis (ETH) [25–27] was proposed. The ETH dictates that observables in the energy eigenbasis have thermal diagonal elements with exponentially small off-diagonal fluctuations. While several exceptions such as many-body localization [11, 17, 28, 29], quantum many-body scars [13, 23, 30, 31], and Hilbert space fragmentation [14, 24, 32, 33] have been discovered, the validity of the ETH in nonintegrable systems has widely been confirmed numerically [34–40].

While the ETH guarantees thermalization in the infinite-time limit, it leaves the finite-time dynamics [41–46] largely unconstrained. In fact, the ETH does not rule out a “burst”—a transient deviation of an expectation value of an observable from its thermal equilibrium value—which is in sharp contrast to usual monotonic thermalization observed in experiments [8, 12, 16, 21, 22].

A burst can arise from fine-tuned initial states by exploiting the time-reversed evolution [46, 47]; however, these states generally have high entanglement, so such a burst does not provide insights into macroscopic irreversibility from low-complexity initial conditions. A related phenomenon is quantum recurrence [48, 49]; however, the recurrence time is typically double-exponential in the system size [50]. The authors of Ref. [51] pointed

out that the ETH itself does not exclude anomalous relaxation dynamics including a burst by constructing specially designed observables; however, whether such “an overlooked loophole” [51] in the ETH exists for local Hamiltonians and observables requires further investigation. The experimental realization of the above three possibilities remains challenging due to high-entangled initial states, extremely long timescales, or nonlocality of Hamiltonians and observables.

In this Letter, we demonstrate that a burst phenomenon of average magnetization can be created at a designated time from a low-entangled initial state for a nonintegrable mixed-field Ising chain (see Fig. 1). We focus on matrix product states (MPSs) [52, 53] in one-dimensional quantum systems as an operationally accessible candidate for such low-entangled states, and utilize the density matrix renormalization group (DMRG) algorithm [54–57] to search for an MPS that creates a burst. This method enables us to create a tailor-made burst for a given Hamiltonian and observable at a designated time. We also find a slow or even negative entanglement growth before the burst time.

We numerically show that for a fixed and short burst time, a bond dimension independent of the system size is sufficient to create a large burst even for a large system. This implies that the burst is experimentally realizable via quantum quenches from ground states [53, 58–60] or shallow quantum circuits [61–64]. Conversely, our analytical argument based on a local random quantum circuit [65] gives a probabilistic no-go result in the long-time regime: as the burst time grows faster than the system size, a burst becomes exponentially rare. Our method allows us to quantitatively evaluate the maximal transient deviation from equilibrium accessible via low-entangled initial states. Such a deviation persists until being overwhelmed by quantum scrambling, even in generic systems that eventually thermalize—a prediction testable with programmable quantum simulators.

* yamada@cat.phys.s.u-tokyo.ac.jp

† hokkyo@cat.phys.s.u-tokyo.ac.jp

‡ ueda@phys.s.u-tokyo.ac.jp

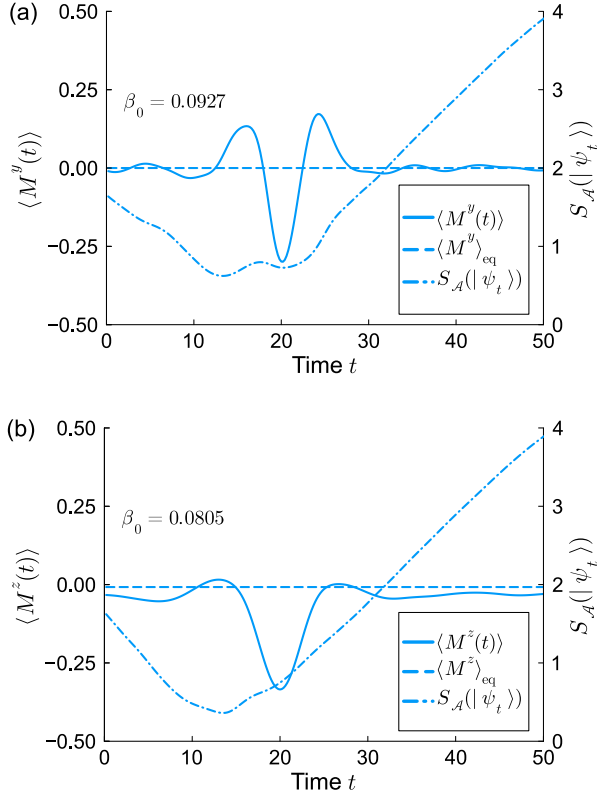


FIG. 1. Time evolution of the expectation value $\langle O(t) \rangle$ (solid) and that of entanglement entropy $S_{\mathcal{A}}(t)$ (dash-dotted, calculated for the half system $\mathcal{A} = \{1, 2, \dots, [L/2]\}$) with $L = 40$ for the mixed-field Ising chain (2). A dashed line indicates the thermal equilibrium value of O . Initial states are obtained by Method 2 with $\tau = 20$, $\chi = 10$, $\beta = 0.1$, and $\lambda_L = 72/L^2$. (a) Case of $O = M^y$. (b) Case of $O = M^z$. Note that $\langle M^z(t) \rangle_{\text{eq}}$ is slightly below zero.

Methods for creating a burst—We consider L sites $\{1, 2, \dots, L\}$ on a one-dimensional chain with the open boundary condition. An MPS can be expressed as $|\psi\rangle = \sum_{\{\sigma_i\}} A_1^{\sigma_1} A_2^{\sigma_2} \dots A_L^{\sigma_L} |\sigma_1 \sigma_2 \dots \sigma_L\rangle$, where σ_i denotes a state of site i and $A_i^{\sigma_i}$ is a $D_i \times D_{i+1}$ matrix with $D_1 = D_{L+1} = 1$. Entanglement entropy for a subsystem \mathcal{A} is defined as $S_{\mathcal{A}}(|\psi\rangle) := -\text{Tr}[\rho_{\mathcal{A}} \ln \rho_{\mathcal{A}}]$ with $\rho_{\mathcal{A}} = \text{Tr}_{\mathcal{A}^c} [|\psi\rangle \langle \psi|]$, where \mathcal{A}^c denotes the complement of \mathcal{A} . Then, the bond dimension $\chi := \max_i D_i$ gives an upper bound on entanglement entropy: $S_{\mathcal{A}}(|\psi\rangle) \leq \ln \chi$ holds for any subsystem $\mathcal{A} = \{1, 2, \dots, i\}$.

We investigate a burst phenomenon starting from an MPS with a bond dimension independent of the system size L . This choice ensures physical relevance: such an MPS is the exact ground state of a local Hamiltonian [53], and can be approximately prepared by a shallow quantum circuit [61–63] (see End Matter for details).

Now, let H , O , τ be a Hamiltonian, a local observable, and a burst time, respectively. We denote $O(t) := e^{iHt} O e^{-iHt}$ as a time-evolved observable in the Heisen-

berg picture. We use the Trotter decomposition [66, 67] to compute the time evolution and the thermal equilibrium value. To secure computational feasibility, the bond dimension of an MPS or a matrix product operator (MPO) [68, 69] is truncated at each Trotter step. Truncating the MPO of $O(t)$ at each Trotter step is justified for short times due to the locality of O [70]. We perform numerical calculations using the ITensor library [71, 72], and confirm that the truncation errors in our setup are indeed small [73].

The simplest method (Method 1) for creating a burst of O at $t = \tau$ is as follows: we compute the state $e^{iH\tau} |\Psi_{\text{GS}}\rangle$ via the time-reversed evolution starting from (one of) the ground state(s) $|\Psi_{\text{GS}}\rangle$ of O , and obtain an initial MPS by truncating this state to a bond dimension χ . Method 1 is computationally efficient and applied to infinite systems (see End Matter for details). However, it lacks control over the energy and its fluctuation. Furthermore, since Method 1 relies on a heuristic truncation, it generally yields a smaller burst compared with the direct optimization of the expectation value $\langle O(\tau) \rangle$. Taking these into account, we introduce the second method (Method 2), which employs the DMRG algorithm.

In Method 2, we consider the following cost function:

$$H_{\text{DMRG}} = O(\tau) + \lambda_L (H - \langle H \rangle_{\beta})^2. \quad (1)$$

Here, $\lambda_L (\geq 0)$ is a system-size dependent penalty weight and $\langle X \rangle_{\beta} := \text{Tr}[X e^{-\beta H}] / \text{Tr}[e^{-\beta H}]$ denotes the thermal equilibrium value of X at the inverse temperature β . The cost function H_{DMRG} is designed to minimize the expectation value $\langle O(\tau) \rangle$ while suppressing the energy fluctuation around a target energy $\langle H \rangle_{\beta}$.

The algorithm of Method 2 is as follows:

1. Compute the cost function (1) as an MPO.
2. Perform the DMRG optimization on the cost function (1) with a bond dimension of at most χ , and obtain an MPS $|\psi_0\rangle$.
3. Determine the inverse temperature β_0 from the condition $\langle H \rangle_{\beta_0} = \langle \psi_0 | H | \psi_0 \rangle$ and obtain the thermal equilibrium value $\langle O \rangle_{\text{eq}} := \langle O \rangle_{\beta_0}$.
4. Compute the time evolution $|\psi_t\rangle = e^{-iHt} |\psi_0\rangle$ and obtain a burst amplitude $\langle O \rangle_{\text{eq}} - \langle O(\tau) \rangle$.

The DMRG algorithm is usually used for finding the ground state of a local Hamiltonian; however, we utilize it to find the MPS that minimizes the expectation value of a nonlocal cost function with a restriction of a bond dimension.

Method 2 enables us to systematically obtain a tailor-made initial MPS that creates a burst under given conditions, and is used for the finite-size scaling analysis performed in the main text of this Letter. This approach allows for explicit control over the target energy and its fluctuation via β and λ_L including the case of $\lambda_L = 0$, which generally yields a larger burst amplitude than Method 1. Here, we judiciously choose a positive λ_L to keep β_0 close to β while simultaneously creating

a burst comparable to or even larger than that obtained by Method 1 [74].

Burst phenomenon—We demonstrate a burst phenomenon for a mixed-field Ising chain:

$$H = \sum_{i=1}^{L-1} J_z S_i^z S_{i+1}^z + \sum_{i=1}^L (h_x S_i^x + h_z S_i^z). \quad (2)$$

Here, $S_i^{x,y,z}$ is a spin-1/2 operator at site i , and we set the parameters as $(J_z, 2h_x, 2h_z) = (1.0, 0.9045, 0.8090)$. The nonintegrability, or chaotic nature, of this model has been verified both numerically [35, 75, 76] and analytically [77, 78]. We follow Method 2 and set $\beta = 0.1$ for a finite system size.

As an observable O we focus on the average magnetization $M^\alpha = \sum_{i=1}^L S_i^\alpha / L$ ($\alpha = y, z$). For the case of $O = M^y$, diagonal elements with respect to the energy eigenbasis vanish due to time-reversal symmetry. Therefore, its thermal equilibrium value is always zero and the diagonal ETH trivially holds.

For the above Hamiltonian and observables, burst phenomena with $L = 40$ are illustrated in Fig. 1, with $O = M^y$ and $O = M^z$ for (a) and (b), respectively. The expectation value of each observable shows a strong peak at the designated time $\tau = 20$. This sudden burst arises from an MPS of bond dimension $\chi = 10$, which is much smaller than typical volume-law states with $\chi \simeq 2^{L/2} \simeq 10^6$. This indicates that the initial state is a simple state with low entanglement, thereby supporting the accessibility of the burst by a quantum quench.

Crucially, bipartite entanglement entropy shows a slow or even negative increase before the burst time in contrast to a typical linear growth [75, 79]. This suggests that local information of the system is temporarily retained in the sense that the reduced density operator of the quantum state remains far from the Gibbs state.

Numerical analysis of a burst amplitude—We investigate how the burst amplitude $\langle O \rangle_{\text{eq}} - \langle O(\tau) \rangle$ depends on the burst time τ under the Hamiltonian (2) with a fixed bond dimension $\chi = 10$. We vary the system size L and follow Method 2 for each L and τ . We set $\lambda_L \propto L^{-2}$ since the spectral widths Δ_O ($O = M^y, M^z$) do not depend on L while Δ_{H^2} scales approximately as L^2 .

The result in the above setting is shown in Fig. 2. It shows that the burst amplitude for a fixed τ remains large with increasing L , especially for a small τ ($\tau \lesssim 20$ for M^y and $\tau \lesssim 18$ for M^z) where a larger L leads to a larger burst. This suggests that a large burst can arise on a short-time scale from an MPS with a fixed bond dimension even when the system size is large. In End Matter, we demonstrate that a burst survives in the thermodynamic limit $L \rightarrow \infty$.

The entire time window analyzed here falls within the regime where operator entanglement entropy of the unitary $e^{-iH\tau}$ grows linearly [76]. Despite this continuous growth of complexity, the burst amplitude remains nearly

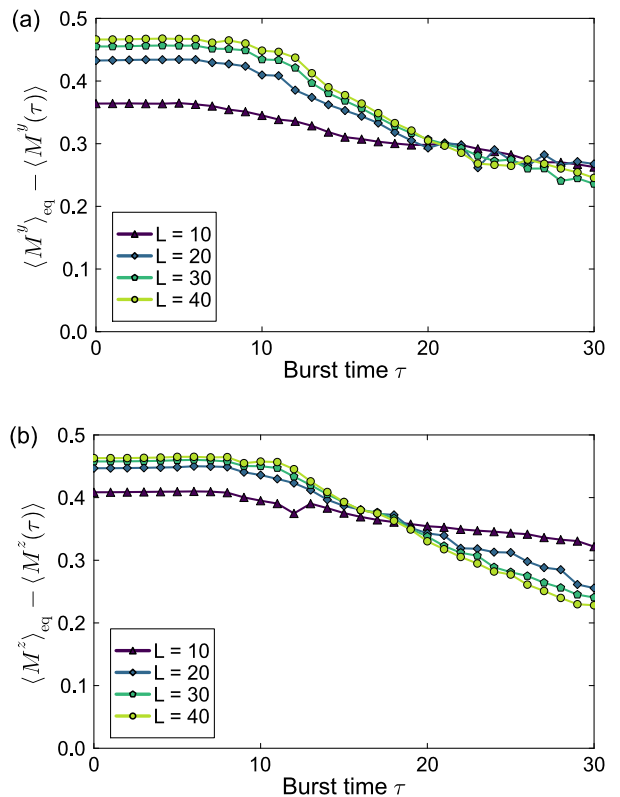


FIG. 2. Burst amplitude $\langle O \rangle_{\text{eq}} - \langle O(\tau) \rangle$ versus the burst time τ with respect to different system sizes L for the mixed-field Ising chain (2). Initial states are obtained by Method 2 with $\chi = 10$, $\beta = 0.1$, and $\lambda_L = 72/L^2$. (a) Case of $O = M^y$. (b) Case of $O = M^z$.

constant for $\tau \lesssim 11$. This suggests that an appropriately chosen initial state can retain local information even amidst ballistic quantum scrambling. The subsequent gradual decay of the burst amplitude suggests that the complexity of the eigenstates of $O(\tau)$ with low eigenvalues eventually exceeds the representational capacity of an MPS as τ increases, marking the crossover region beyond which scrambling becomes dominant.

Evaluation by a local random circuit—We return to a more general case with a one-dimensional chain of L sites, each of which has a local dimension d . Here, we consider a random unitary evolution U which follows a measure $\nu_{d,L}^{*s}$, where in each of the s steps an index i is chosen at random from $\{1, 2, \dots, L-1\}$, and a unitary $U_{i,i+1}$ drawn from the Haar measure on $\mathbb{U}(d^2)$ acts upon qudits i and $i+1$ [65]. This setting is to approximate the time evolution by a random time-dependent, 2-local (nearest-neighbor interaction) Hamiltonian [80]. Since generic random circuits do not conserve energy, the system thermalizes toward the infinite-temperature state. Therefore, we quantify the burst amplitude as the deviation from the infinite-temperature average $\langle O \rangle_{\beta=0} = \text{Tr}[O]/d^L$.

First, we consider a burst starting from a fixed initial state $|\psi\rangle$. In this local random circuit, the probability that the burst is larger than or equal to $\Delta_O a$ is bounded from above as follows [65, 81–83]:

$$\Pr_{U \sim \nu_{d,L}^{*,s}} \left[\left| \langle \psi | U^\dagger O U | \psi \rangle - \frac{\text{Tr}[O]}{d^L} \right| \geq \Delta_O a \right] \leq 2 \left(\frac{m}{d^L a^2} \right)^m, \\ \mathbb{Z}_{\geq 0} \ni m \leq \frac{k}{2}, \quad k = \left\lfloor \left(\frac{s}{C L^2 d^2 \ln d} \right)^{1/11} \right\rfloor, \quad (3)$$

where C is a positive numerical constant. (The proofs for Eqs. (3) and (5) are given in Supplemental Material.) This inequality reflects the concentration of measure induced by approximate unitary k -designs, which improves as the number of gates s increases [65].

We extend this bound in Eq. (3) to the entire manifold \mathcal{M}_χ of normalized MPSs whose bond dimensions are less than or equal to χ . We denote

$$P_{\chi,a} := \Pr_{U \sim \nu_{d,L}^{*,s}} \sup_{|\psi\rangle \in \mathcal{M}_\chi} \left[\left| \langle \psi | U^\dagger O U | \psi \rangle - \frac{\text{Tr}[O]}{d^L} \right| \geq \Delta_O a \right] \quad (4)$$

as the probability of finding a burst from a state in \mathcal{M}_χ . For a bond dimension χ which is independent of L , the logarithm of $P_{\chi,a}$ is approximately bounded as

$$\ln P_{\chi,a} \lesssim -m \ln(m d^L) + 2(d L \chi^2 + m) \ln \frac{d L \chi^2 + m}{a}. \quad (5)$$

In the local random circuit, the total number of gates s should be proportional to the system size L and the time τ to imitate the time evolution by a 2-local Hamiltonian. Then, $k \simeq C'(\tau/L)^{1/11}$ holds for $\tau \gg L$, where C' is a constant which depends only on d .

The asymptotic behavior of the right-hand side of Eq. (5) is summarized in Table I. This quantity does not decay with L for $\tau \ll L(\ln L)^{11}$, which is interpreted as an upper bound on the time scale of a stable burst. For $L(\ln L)^{11} \ll \tau \ll L d^{11L}$, the upper bound of $P_{\chi,a}$ decays exponentially with $L^{10/11} \tau^{1/11}$. For $L d^{11L} \ll \tau$, $m \simeq d^L a^2 / e$ gives a tighter bound than $m \simeq k/2$, and the upper bound decays double-exponentially with L . These results altogether suggest that in the long-time regime, a large burst cannot be created from any MPS for most time-dependent local Hamiltonians.

We have employed local random circuits to leverage rigorous results of approximate k -designs, noting that this setting corresponds to time-dependent Hamiltonians. However, our burst-creating methods are still applicable even in the time-dependent setting. Provided that similar rigorous bounds can be established for circuits with symmetries [84–86]—and ultimately extended to energy conservation—the probabilistic evaluation of a burst would follow analogously. We could also establish a similar bound on entanglement entropy by using the concentration of measure for approximate k -designs [65, 81].

Discussion—We have demonstrated a burst phenomenon of average magnetization starting from a low-entangled state for a nonintegrable mixed-field Ising

TABLE I. Choice of m and the leading term (LT) on the right-hand side of Eq. (5) for different regions of the burst time τ . The integer m is chosen to satisfy $m \leq k/2$, where $k \simeq C'(\tau/L)^{1/11}$ holds for some constant C' when $\tau \gg L$.

τ	m	LT in Eq. (5)
$\tau \ll L(\ln L)^{11}$	$\lesssim \frac{C'}{2} \left(\frac{\tau}{L} \right)^{1/11}$	$2dL\chi^2 \ln L$
$L(\ln L)^{11} \ll \tau \ll L d^{11L}$	$\simeq \frac{C'}{2} \left(\frac{\tau}{L} \right)^{1/11} - \frac{C'}{2} L^{10/11} \tau^{1/11} \ln d$	
$L d^{11L} \ll \tau$	$\simeq \frac{d^L a^2}{e} - \frac{d^L a^2}{e}$	

chain. By utilizing the DMRG algorithm, we have identified an MPS that creates a large burst at a designated time. We have found that in the short-time regime when quantum scrambling sets in, a large burst accompanied by a slow or even negative entanglement growth arises from an MPS with a fixed bond dimension even for a large system. This means that the burst from a low-entangled initial state can be realized by a quantum quench. Conversely, at long times, the burst amplitude becomes small, which is consistent with our analytical bounds derived from local random circuits. Our results suggest that starting from an appropriately chosen low-entangled state—rather than a typical one—allows the system to stay out of equilibrium for a prolonged time. However, the state is eventually overwhelmed by growing quantum scrambling, which drives the system into equilibrium.

A burst can be regarded as a transient defiance against thermalization: even if a local observable satisfies the ETH and initially takes its expectation value near the thermal equilibrium value, it can subsequently exhibit a deviation accompanied by an anomalous suppression of entanglement entropy. We have shown that such an exotic phenomenon can arise from low-entangled states that can be systematically constructed for generic local Hamiltonians and observables. Moreover, we expect that our variational method can be adapted to target other nonequilibrium trajectories—such as revival and oscillation—by modifying the cost function. Such studies may offer insights into quantum thermalization beyond the infinite-time limit.

An interesting question regarding a burst is whether it happens when a system includes long-range interactions. We expect that a burst decays faster due to stronger quantum scrambling; however, it has yet to be confirmed for large systems due to computational cost. Such a study may shed new light on how locality of interactions affects thermalization processes.

A burst phenomenon offers a potential avenue for quantum metrology. The burst amplitude of an intensive observable remains $\mathcal{O}(L^0)$ unlike thermal fluctuations, which are suppressed as $\mathcal{O}(L^{-1/2})$. This high signal-to-

noise ratio could be exploited in quantum sensors and simulators: by comparing the precalculated theoretical predictions with experimental results, one could estimate system parameters or benchmark the performance of quantum simulators.

Acknowledgments—We thank Masaya Nakagawa for fruitful discussions and giving the “burst” its name. We also thank Shion Yamashita for encouraging us to use iMPSs for the analysis in the thermodynamics limit. S. Y. and A. H. were supported by Forefront Physics and Mathematics Program to Drive Transformation (FoPM), a World-leading Innovative Graduate Study (WINGS) Program, the University of Tokyo. A. H. was also sup-

ported by KAKENHI Grant No. JP25KJ0833 from the Japan Society for the Promotion of Science (JSPS) and JSR Fellowship, the University of Tokyo. M. U. was supported by KAKENHI Grant No. JP22H01152 from the JSPS. We gratefully acknowledge the support from the CREST program “Quantum Frontiers” (Grant No. JPMJCR23I1) by the Japan Science and Technology Agency (JST). This work was supported by JST as part of Adopting Sustainable Partnerships for Innovative Research Ecosystem (ASPIRE), Grant No. JPMJAP25A1.

Data availability—The data that support the findings of this article are available upon reasonable request.

[1] J. v. Neumann, Beweis des Ergodensatzes und des H -Theorems in der neuen Mechanik, *Zeitschrift für Physik* **57**, 30 (1929).

[2] A. Polkovnikov, K. Sengupta, A. Silva, and M. Vengalattore, *Colloquium: Nonequilibrium dynamics of closed interacting quantum systems*, *Reviews of Modern Physics* **83**, 863 (2011).

[3] J. Eisert, M. Friesdorf, and C. Gogolin, Quantum many-body systems out of equilibrium, *Nature Physics* **11**, 124 (2015).

[4] C. Gogolin and J. Eisert, Equilibration, thermalisation, and the emergence of statistical mechanics in closed quantum systems, *Reports on Progress in Physics* **79**, 056001 (2016).

[5] L. D’Alessio, Y. Kafri, A. Polkovnikov, and M. Rigol, From quantum chaos and eigenstate thermalization to statistical mechanics and thermodynamics, *Advances in Physics* **65**, 239 (2016).

[6] T. Mori, T. N. Ikeda, E. Kaminishi, and M. Ueda, Thermalization and prethermalization in isolated quantum systems: a theoretical overview, *Journal of Physics B: Atomic, Molecular, and Optical Physics* **51**, 112001 (2018).

[7] T. Kinoshita, T. Wenger, and D. S. Weiss, A quantum Newton’s cradle, *Nature* **440**, 900 (2006).

[8] S. Trotzky, Y. A. Chen, A. Flesch, I. P. McCulloch, and others, Probing the relaxation towards equilibrium in an isolated strongly correlated one-dimensional Bose gas, *Nature Physics* **8**, 325 (2012).

[9] M. Gring, M. Kuhnert, T. Langen, T. Kitagawa, B. Rauer, M. Schreitl, I. Mazets, D. A. Smith, E. Demler, and J. Schmiedmayer, Relaxation and prethermalization in an isolated quantum system, *Science* **337**, 1318 (2012).

[10] T. Langen, R. Geiger, M. Kuhnert, B. Rauer, and J. Schmiedmayer, Local emergence of thermal correlations in an isolated quantum many-body system, *Nature Physics* **9**, 640 (2013).

[11] M. Schreiber, S. S. Hodgman, P. Bordia, H. P. Lüschen, M. H. Fischer, R. Vosk, E. Altman, U. Schneider, and I. Bloch, Observation of many-body localization of interacting fermions in a quasirandom optical lattice, *Science* **349**, 842 (2015).

[12] A. M. Kaufman, M. E. Tai, A. Lukin, M. Rispoli, R. Schittko, P. M. Preiss, and M. Greiner, Quantum thermalization through entanglement in an isolated many-body system, *Science* **353**, 794 (2016).

[13] H. Bernien, S. Schwartz, A. Keesling, H. Levine, A. Omran, H. Pichler, S. Choi, A. Zibrov, M. Endres, M. Greiner, V. Vuletić, and M. Lukin, Probing many-body dynamics on a 51-atom quantum simulator, *Nature* **551**, 579 (2017).

[14] S. Scherg, T. Kohlert, P. Sala, F. Pollmann, B. Hebbe Madhusudhana, I. Bloch, and M. Aidelsburger, Observing non-ergodicity due to kinetic constraints in tilted Fermi-Hubbard chains, *Nature Communications* **12**, 4490 (2021).

[15] P. Richerme, Z.-X. Gong, A. Lee, C. Senko, J. Smith, M. Foss-Feig, S. Michalakis, A. V. Gorshkov, and C. Monroe, Non-local propagation of correlations in quantum systems with long-range interactions, *Nature* **511**, 198 (2014).

[16] G. Clos, D. Porras, U. Warring, and T. Schaetz, Time-resolved observation of thermalization in an isolated quantum system, *Physical Review Letters* **117**, 170401 (2016).

[17] J. Smith, A. Lee, P. Richerme, B. Neyenhuis, P. W. Hess, P. Hauke, M. Heyl, D. A. Huse, and C. Monroe, Many-body localization in a quantum simulator with programmable random disorder, *Nature Physics* **12**, 907 (2016).

[18] B. Neyenhuis, J. Zhang, P. W. Hess, J. Smith, A. C. Lee, P. Richerme, Z.-X. Gong, A. V. Gorshkov, and C. Monroe, Observation of prethermalization in long-range interacting spin chains, *Science Advances* **3**, e1700672 (2017).

[19] C. Neill, P. Roushan, M. Fang, Y. Chen, M. Kolodrubetz, Z. Chen, A. Megrant, R. Barends, B. Campbell, B. Chiaro, A. Dunsworth, E. Jeffrey, J. Kelly, J. Mutus, P. J. O’Malley, C. Quintana, D. Sank, A. Vainsencher, J. Wenner, T. C. White, A. Polkovnikov, and J. M. Martinis, Ergodic dynamics and thermalization in an isolated quantum system, *Nature Physics* **12**, 1037 (2016).

[20] M. S. Blok, V. V. Ramasesh, T. Schuster, K. O’Brien, J. M. Kreikebaum, D. Dahmen, A. Morvan, B. Yoshida, N. Y. Yao, and I. Siddiqi, Quantum information scrambling on a superconducting qutrit processor, *Physical Review X* **11**, 021010 (2021).

[21] F. Chen, Z.-H. Sun, M. Gong, Q. Zhu, Y.-R. Zhang, Y. Wu, Y. Ye, C. Zha, S. Li, S. Guo, H. Qian, H.-L.

Huang, J. Yu, H. Deng, H. Rong, J. Lin, Y. Xu, L. Sun, C. Guo, N. Li, F. Liang, C.-Z. Peng, H. Fan, X. Zhu, and J.-W. Pan, Observation of strong and weak thermalization in a superconducting quantum processor, *Physical Review Letters* **127**, 020602 (2021).

[22] Q. Zhu, Z.-H. Sun, M. Gong, F. Chen, Y.-R. Zhang, Y. Wu, Y. Ye, C. Zha, S. Li, S. Guo, H. Qian, H.-L. Huang, J. Yu, H. Deng, H. Rong, J. Lin, Y. Xu, L. Sun, C. Guo, N. Li, F. Liang, C.-Z. Peng, H. Fan, X. Zhu, and J.-W. Pan, Observation of thermalization and information scrambling in a superconducting quantum processor, *Physical Review Letters* **128**, 160502 (2022).

[23] P. Zhang, H. Dong, Y. Gao, L. Zhao, J. Hao, J.-Y. Desaules, Q. Guo, J. Chen, J. Deng, B. Liu, W. Ren, Y. Yao, X. Zhang, S. Xu, K. Wang, F. Jin, X. Zhu, B. Zhang, H. Li, C. Song, Z. Wang, F. Liu, Z. Papić, L. Ying, H. Wang, and Y.-C. Lai, Many-body Hilbert space scar-ring on a superconducting processor, *Nature Physics* **19**, 120 (2022).

[24] Y.-Y. Wang, Y.-H. Shi, Z.-H. Sun, C.-T. Chen, Z.-A. Wang, K. Zhao, H.-T. Liu, W.-G. Ma, Z. Wang, H. Li, J.-C. Zhang, Y. Liu, C.-L. Deng, T.-M. Li, Y. He, Z.-H. Liu, Z.-Y. Peng, X. Song, G. Xue, H. Yu, K. Huang, Z. Xiang, D. Zheng, K. Xu, and H. Fan, Exploring Hilbert-space fragmentation on a superconducting processor, *PRX Quantum* **6**, 010325 (2025).

[25] J. M. Deutsch, Quantum statistical mechanics in a closed system, *Physical Review A* **43**, 2046 (1991).

[26] M. Srednicki, Chaos and quantum thermalization, *Physical Review E* **50**, 888 (1994).

[27] M. Rigol, V. Dunjko, and M. Olshanii, Thermalization and its mechanism for generic isolated quantum systems, *Nature* **452**, 854 (2008).

[28] D. M. Basko, I. L. Aleiner, and B. L. Altshuler, Metal-insulator transition in a weakly interacting many-electron system with localized single-particle states, *Annals of Physics* **321**, 1126 (2006).

[29] J. Z. Imbrie, On many-body localization for quantum spin chains, *Journal of Statistical Physics* **163**, 998 (2016).

[30] N. Shiraishi and T. Mori, Systematic construction of counterexamples to the eigenstate thermalization hypothesis, *Physical Review Letters* **119**, 030601 (2017).

[31] S. Moudgalya, S. Rachel, B. Andrei Bernevig, and N. Regnault, Exact excited states of nonintegrable models, *Physical Review B* **98**, 235155 (2018).

[32] P. Sala, T. Rakovszky, R. Verresen, M. Knap, and F. Pollmann, Ergodicity breaking arising from Hilbert space fragmentation in dipole-conserving Hamiltonians, *Physical Review X* **10**, 011047 (2020).

[33] V. Khemani, M. Hermele, and R. Nandkishore, Localization from Hilbert space shattering: From theory to physical realizations, *Physical Review B* **101**, 174204 (2020).

[34] R. Steinigeweg, J. Herbrych, and P. Prelovšek, Eigenstate thermalization within isolated spin-chain systems, *Physical Review E* **87**, 012118 (2013).

[35] H. Kim, T. N. Ikeda, and D. A. Huse, Testing whether all eigenstates obey the eigenstate thermalization hypothesis, *Physical Review E* **90**, 052105 (2014).

[36] W. Beugeling, R. Moessner, and M. Haque, Finite-size scaling of eigenstate thermalization, *Physical Review E* **89**, 042112 (2014).

[37] W. Beugeling, R. Moessner, and M. Haque, Off-diagonal matrix elements of local operators in many-body quantum systems, *Physical Review E* **91**, 012144 (2015).

[38] R. Mondaini and M. Rigol, Eigenstate thermalization in the two-dimensional transverse field Ising model. II. Off-diagonal matrix elements of observables, *Physical Review E* **96**, 012157 (2017).

[39] J. R. Garrison and T. Grover, Does a single eigenstate encode the full Hamiltonian?, *Physical Review X* **8**, 021026 (2018).

[40] S. Sugimoto, R. Hamazaki, and M. Ueda, Test of the eigenstate thermalization hypothesis based on local random matrix theory, *Physical Review Letters* **126**, 120602 (2021).

[41] J. Berges, S. Borsányi, and C. Wetterich, Prethermalization, *Physical Review Letters* **93**, 142002 (2004).

[42] C. Bartsch and J. Gemmer, Dynamical typicality of quantum expectation values, *Physical Review Letters* **102**, 110403 (2009).

[43] M. C. Bañuls, J. I. Cirac, and M. B. Hastings, Strong and weak thermalization of infinite nonintegrable quantum systems, *Physical Review Letters* **106**, 050405 (2011).

[44] A. J. Short and T. Farrelly, Quantum equilibration in finite time, *New Journal of Physics* **14**, 013063 (2011).

[45] S. Goldstein, T. Hara, and H. Tasaki, Time scales in the approach to equilibrium of macroscopic quantum systems, *Physical Review Letters* **111**, 140401 (2013).

[46] A. Dymarsky, Mechanism of macroscopic equilibration of isolated quantum systems, *Physical Review B* **99**, 224302 (2019).

[47] A. Peres, Stability of quantum motion in chaotic and regular systems, *Physical Review A* **30**, 1610 (1984).

[48] P. Bocchieri and A. Loinger, Quantum Recurrence Theorem, *Physical Review* **107**, 337 (1957).

[49] I. C. Percival, Almost periodicity and the quantal H theorem, *Journal of Mathematical Physics* **2**, 235 (1961).

[50] A. Peres, Recurrence phenomena in quantum dynamics, *Physical Review Letters* **49**, 1118 (1982).

[51] L. Knipschild and J. Gemmer, Modern concepts of quantum equilibration do not rule out strange relaxation dynamics, *Physical Review E* **101**, 062205 (2020).

[52] M. Fannes, B. Nachtergael, and R. F. Werner, Finitely correlated states on quantum spin chains, *Communications in Mathematical Physics* **144**, 443 (1992).

[53] D. Perez-Garcia, F. Verstraete, M. M. Wolf, and J. I. Cirac, Matrix product state representations, *Quantum Information & Computation* **7**, 401 (2007).

[54] S. R. White, Density matrix formulation for quantum renormalization groups, *Physical Review Letters* **69**, 2863 (1992).

[55] S. R. White, Density-matrix algorithms for quantum renormalization groups, *Physical Review B* **48**, 10345 (1993).

[56] Ü. Schollwöck, The density-matrix renormalization group, *Reviews of Modern Physics* **77**, 259 (2005).

[57] Ü. Schollwöck, The density-matrix renormalization group in the age of matrix product states, *Annals of Physics* **326**, 96 (2011).

[58] F. Verstraete and J. I. Cirac, Matrix product states represent ground states faithfully, *Physical Review B* **73**, 094423 (2006).

[59] M. B. Hastings, An area law for one-dimensional quan-

tum systems, *Journal of Statistical Mechanics: Theory and Experiment* **2007**, P08024 (2007).

[60] P. Sompet, S. Hirthe, D. Bourgund, T. Chalopin, J. Bibo, J. Koepsell, P. Bojović, R. Verresen, F. Pollmann, G. Salomon, C. Gross, T. A. Hilker, and I. Bloch, Realizing the symmetry-protected Haldane phase in Fermi-Hubbard ladders, *Nature* **606**, 484 (2022).

[61] S.-J. Ran, Encoding of matrix product states into quantum circuits of one- and two-qubit gates, *Physical Review A* **101**, 032310 (2020).

[62] T. Shirakawa, H. Ueda, and S. Yunoki, Automatic quantum circuit encoding of a given arbitrary quantum state, *Physical Review Research* **6**, 043008 (2024).

[63] M. S. Rudolph, J. Chen, J. Miller, A. Acharya, and A. Perdomo-Ortiz, Decomposition of matrix product states into shallow quantum circuits, *Quantum Science and Technology* **9**, 015012 (2024).

[64] J. Iaconis, S. Johri, and E. Y. Zhu, Quantum state preparation of normal distributions using matrix product states, *npj Quantum Information* **10**, 15 (2024).

[65] F. G. S. L. Brandão, A. W. Harrow, and M. Horodecki, Local random quantum circuits are approximate polynomial-designs, *Communications in Mathematical Physics* **346**, 397 (2016).

[66] H. F. Trotter, On the product of semi-groups of operators, *Proceedings of the American Mathematical Society* **10**, 545 (1959).

[67] M. Suzuki, Generalized Trotter's formula and systematic approximants of exponential operators and inner derivations with applications to many-body problems, *Communications in Mathematical Physics* **51**, 183 (1976).

[68] F. Verstraete, J. J. García-Ripoll, and J. I. Cirac, Matrix product density operators: simulation of finite-temperature and dissipative systems, *Physical Review Letters* **93**, 207204 (2004).

[69] B. Pirvu, V. Murg, J. I. Cirac, and F. Verstraete, Matrix product operator representations, *New Journal of Physics* **12**, 025012 (2010).

[70] Á. M. Alhambra and J. I. Cirac, Locally accurate tensor networks for thermal states and time evolution, *PRX Quantum* **2**, 040331 (2021).

[71] M. Fishman, S. R. White, and E. M. Stoudenmire, The ITensor software library for tensor network calculations, *SciPost Physics Codebases* **4** (2022).

[72] M. Fishman, S. R. White, and E. M. Stoudenmire, Codebase release 0.3 for ITensor, *SciPost Physics Codebases* **4–r0.3** (2022).

[73] We perform Step 1 of Method 2 with the maximum bond dimension of 2^{11} . For $L = 10, 20, 30$, and 40 , the truncation error defined by $\epsilon_O(\tau) := 1 - (\|O(\tau)\|_F / \|O\|_F)^2$ under the Hamiltonian (2) satisfies $\epsilon_O(20) < 6 \times 10^{-4}$ and $\epsilon_O(30) < 10^{-2}$ for $O = M^y, M^z$.

[74] The burst amplitudes obtained by Method 1, Method 2 ($\lambda_L = 0$), and Method 2 ($\lambda_L = 72/L^2$) with $L = 40$, $\tau = 20$, and $\chi = 10$ under the Hamiltonian (2) are 0.222, 0.371, and 0.305 for $O = M^y$, and 0.337, 0.396, and 0.330 for $O = M^z$, respectively.

[75] H. Kim and D. A. Huse, Ballistic spreading of entanglement in a diffusive nonintegrable system, *Physical Review Letters* **111**, 127205 (2013).

[76] T. Zhou and D. J. Luitz, Operator entanglement entropy of the time evolution operator in chaotic systems, *Physical Review B* **95**, 094206 (2017).

[77] X. Cao, A statistical mechanism for operator growth, *Journal of Physics A: Mathematical and Theoretical* **54**, 144001 (2021).

[78] Y. Chiba, Proof of absence of local conserved quantities in the mixed-field Ising chain, *Physical Review B* **109**, 035123 (2024).

[79] P. Calabrese and J. Cardy, Evolution of entanglement entropy in one-dimensional systems, *Journal of Statistical Mechanics: Theory and Experiment* **2005**, P04010 (2005).

[80] D. Poulin, A. Qarry, R. Somma, and F. Verstraete, Quantum simulation of time-dependent Hamiltonians and the convenient illusion of Hilbert space, *Physical Review Letters* **106**, 170501 (2011).

[81] R. A. Low, Large deviation bounds for k -designs, *Proceedings of the Royal Society A* **465**, 3289 (2009).

[82] R. A. Low, *Pseudo-randomness and Learning in Quantum Computation*, Ph.D. thesis, University of Bristol, UK, University of Bristol (2010).

[83] G. Aubrun, J. Jenkins, and S. J. Szarek, Optimal constants in concentration inequalities on the sphere and in the Gauss space, *arXiv:2406.13581 [math.PR]* (2024).

[84] Z. Li, H. Zheng, J. Liu, L. Jiang, and Z.-W. Liu, Designs from local random quantum circuits with $SU(d)$ symmetry, *PRX Quantum* **5**, 040349 (2024).

[85] S. N. Hearth, M. O. Flynn, A. Chandran, and C. R. Laumann, Unitary k -designs from random number-conserving quantum circuits, *Physical Review X* **15**, 021022 (2025).

[86] Y. Mitsuhashi, R. Suzuki, T. Soejima, and N. Yoshikawa, Unitary designs of symmetric local random circuits, *Physical Review Letters* **134**, 180404 (2025).

END MATTER

Preparing initial states with quantum circuits—An initial MPS that creates a burst at a given time can be approximately prepared by a shallow quantum circuit consisting only of neighboring two-qubit gates [61–63]. Here we adopt the Iter[$D_i O_{\text{all}}$] method in Ref. [63] to construct a staircase quantum circuit with K layers (see Fig. 3) that gives an approximate state $|\psi_{\text{app}}\rangle$ of a target MPS $|\psi_0\rangle$.

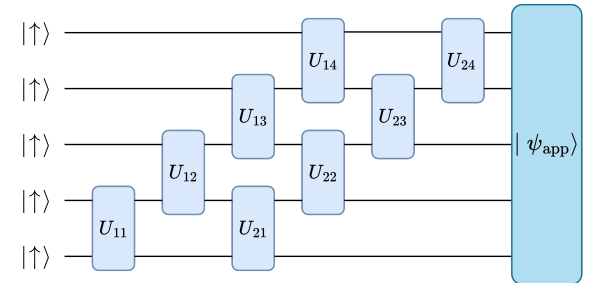


FIG. 3. Schematic illustration of a quantum circuit that creates an approximate MPS $|\psi_{\text{app}}\rangle$ with $L = 5$ spins and $K = 2$ layers.

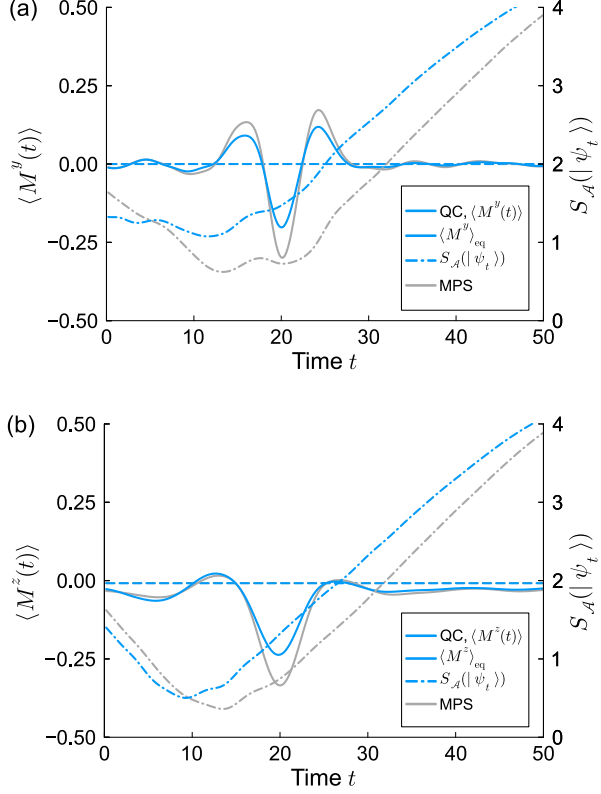


FIG. 4. Comparison of the time evolution between the target MPS $|\psi_0\rangle$ (gray) and its quantum circuit (QC) approximation $|\psi_{\text{app}}\rangle$ (blue) with $L = 40$ for the mixed-field Ising chain (2). A solid curve and a dash-dotted curve represent the time evolution of the expectation value $\langle O(t) \rangle$ and that of entanglement entropy $S_A(t)$ calculated for the half system $\mathcal{A} = \{1, 2, \dots, \lfloor L/2 \rfloor\}$, respectively. For gray curves, initial states are obtained by Method 2 with $\tau = 20$, $\chi = 10$, $\beta = 0.1$, and $\lambda_L = 72/L^2$. For blue curves, initial states are prepared by staircase quantum circuits of $K = 5$ layers that approximate the exact MPSs. (a) Case of $O = M^y$. (b) Case of $O = M^z$.

Figure 4 presents the comparison of bursts starting from two initial states: the exact MPS (gray curves) and the approximate state (blue curves). A burst can still be observed starting from the latter, although the burst amplitude becomes a little smaller. Entanglement entropy still shows a decrease starting from the approximate state in contrast to a typical linear growth; however, the decrease is less pronounced than in the case of the exact MPS.

Burst in the thermodynamic limit—We demonstrate that a burst survives in the thermodynamic limit $L \rightarrow \infty$ by using the infinite matrix product state (iMPS) formalism. Here, we follow Method 1, where we obtain an initial iMPS by truncating $e^{iH\tau} |\Psi_{\text{GS}}\rangle$ with $|\Psi_{\text{GS}}\rangle$ being the ground state of O .

The dependence of a burst amplitude on the burst time

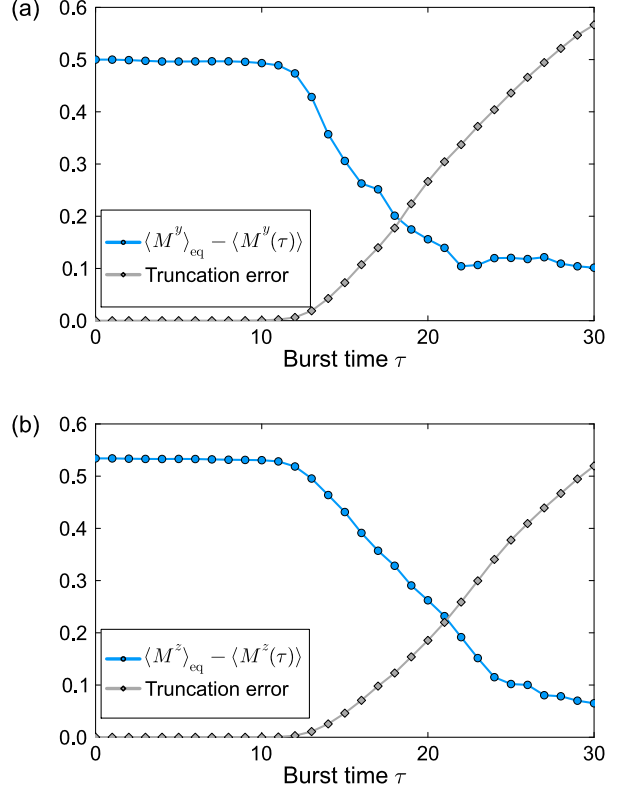


FIG. 5. Burst amplitude $\langle O \rangle_{\text{eq}} - \langle O(\tau) \rangle$ versus the burst time τ in the thermodynamic limit for the mixed-field Ising chain (2). Initial states are obtained by Method 1 with $\chi = 10$, and a gray curve shows the average truncation error of the two bonds in an iMPS. (a) Case of $O = M^y$. (b) Case of $O = M^z$.

is shown in Fig. 5. For a small τ ($\lesssim 11$ for both $O = M^y$ and $O = M^z$), the burst amplitude $\langle O \rangle_{\text{eq}} - \langle O(\tau) \rangle$ is initially large and remains nearly constant. This plateau is consistent with the observation that the state $e^{iH\tau} |\Psi_{\text{GS}}\rangle$ is well approximated by an iMPS of bond dimension $\chi = 10$ in this time regime. Then, the burst amplitude decays gradually for $\tau \gtrsim 11$. This is accompanied by an increase in the truncation error, indicating that $e^{iH\tau} |\Psi_{\text{GS}}\rangle$ becomes increasingly complex, eventually exceeding the representational capacity of an iMPS. These behaviors are similar to the result shown in Fig. 2. Our results demonstrate that a burst is initially robust in the thermodynamic limit, but gradually decays as quantum scrambling becomes stronger.

Supplemental Material

In this Supplemental Material, we derive Eqs. (3) and (5) in the main text for the local dimension $d \geq 2$, the system size $L \geq 2$, and the number of gates $s \geq 1$. By definition, the bond dimension satisfies $\chi \geq 1$.

Appendix A: Concentration of measure for local random circuits: Proof of Eq. (3)

Definition 1 (Definition 1 of [65]). *Let D be the dimension of the Hilbert space, and \mathbf{H} be the Haar measure on $\mathbb{U}(D)$ (the group of $D \times D$ unitary matrices). Then, for a distribution ν on $\mathbb{U}(D)$ and a positive integer $k \in \mathbb{Z}_{>0}$, define*

$$g(\nu, k) := \|\mathbb{E}_{U \sim \nu} U^{\otimes k, k} - \mathbb{E}_{U \sim \mathbf{H}} U^{\otimes k, k}\|_{\infty}, \quad U^{\otimes k, k} := U^{\otimes k} \otimes (U^*)^{\otimes k}. \quad (\text{A1})$$

Lemma 2 (Theorem 5 of [65]). *For $\nu_{d,L}^{*s}$ defined in the main text, the following inequality holds:*

$$g(\nu_{d,L}^{*1}, k) \leq 1 - (42500L \lceil \log_d(4k) \rceil^2 d^2 k^{5+3.1/\ln d})^{-1}. \quad (\text{A2})$$

Lemma 3. *For some positive numerical constant C ,*

$$g(\nu_{d,L}^{*s}, k) \leq d^{-4Lk}, \quad k = \left\lfloor \left(\frac{s}{CL^2 d^2 \ln d} \right)^{1/11} \right\rfloor \quad (\text{A3})$$

holds if $s \geq CL^2 d^2 \ln d$.

Proof. First, there exists a constant C such that

$$C \geq 170000 \{ \log_2(4k) + 1 \}^2 k^{-5+3.1/\ln 2} \quad (\text{A4})$$

holds for all $k \geq 1$. (Note that $C = 2.1 \times 10^6$ is sufficient.) Then, the following inequality holds for $d \geq 2$:

$$\begin{aligned} s &\geq CL^2 d^2 \ln d \cdot k^{11} \\ &\geq 170000L^2 d^2 \ln d \lceil \log_d(4k) \rceil^2 k^{6+3.1/\ln d}. \end{aligned} \quad (\text{A5})$$

It follows from Def. 1 that $g(\nu_{d,L}^{*s}, k) = g(\nu_{d,L}^{*1}, k)^s$ (which is Eq. (3) in Ref. [65]). Using this equation and the inequality $(1-x)^s \leq e^{-sx}$ for $0 \leq x \leq 1$ and $s > 0$, we obtain

$$\begin{aligned} g(\nu_{d,L}^{*s}, k) &\leq \exp \left\{ -s(42500L \lceil \log_d(4k) \rceil^2 d^2 k^{5+3.1/\ln d})^{-1} \right\} \\ &\leq d^{-4Lk}. \end{aligned} \quad (\text{A6})$$

■

Definition 4 (Definition 2.2 of [81]). *A monomial in elements of a unitary matrix U is of degree (k_1, k_2) if it contains k_1 conjugated elements and k_2 unconjugated elements. We call it a balanced monomial of degree k if it is of degree (k, k) . A polynomial is of degree k if it is a sum of balanced monomials of degree at most k .*

Definition 5 (Definition 2.6 of [81]). *ν is an ϵ -approximate unitary k -design if, for all balanced monomials M of degree $\leq k$,*

$$|\mathbb{E}_{\nu} M(U) - \mathbb{E}_{\mathbf{H}} M(U)| \leq \frac{\epsilon}{D^k}. \quad (\text{A7})$$

Lemma 6 (Lemma 2.2.14 of [82]). *When $g(\nu, k) \leq \epsilon$ holds, ν is a $D^{3k} \epsilon$ -approximate k -design.*

Lemma 7 (Theorem 1.2 of [81]). *Let f be a polynomial of degree K . Let us introduce $f(U) = \sum_i \alpha_i M_i(U)$, where $M_i(U)$ are monomials and $\alpha(f) = \sum_i |\alpha_i|$. Suppose that f has the following probability concentration:*

$$\Pr_{U \sim \mathbf{H}} [|f(U) - \mu| \geq \delta] \leq Ae^{-b\delta^2}, \quad (\text{A8})$$

where \mathbf{H} denotes the Haar measure. Let ν be an ϵ -approximate k -design. Then we have

$$\Pr_{U \sim \nu} [|f(U) - \mu| \geq \delta] \leq \delta^{-2m} \left\{ A \left(\frac{m}{b} \right)^m + \frac{\epsilon}{D^k} (\alpha(f) + |\mu|)^{2m} \right\} \quad (\text{A9})$$

for a positive integer m with $2mK \leq k$.

Proposition 8 (Eq. (3) in the main text).

$$\Pr_{U \sim \nu_{d,L}^{*s}} \left[\left| \langle \psi | U^\dagger O U | \psi \rangle - \frac{\text{Tr}[O]}{d^L} \right| \geq \Delta_O a \right] \leq 2 \left(\frac{m}{d^L a^2} \right)^m \quad (\text{A10})$$

holds for an integer $m \in \mathbb{Z}_{\geq 0}$ that satisfies

$$m \leq \frac{k}{2}, \quad k = \left\lfloor \left(\frac{s}{CL^2 d^2 \ln d} \right)^{1/11} \right\rfloor, \quad (\text{A11})$$

where C is the constant defined in Lem. 3.

Proof. Without loss of generality, we assume that O is traceless and $\Delta_O = 1$. By Levy's lemma [83], we have

$$\Pr_{U \sim \text{H}} [\langle \psi | U^\dagger O U | \psi \rangle \geq a] \leq e^{-d^L a^2}. \quad (\text{A12})$$

We introduce $f_O(U) = \langle \psi | U^\dagger O U | \psi \rangle$ and apply Lem. 7 with $D = d^L$, $K = 1$, and $\mu = 0$. Also, $\alpha(f_O) = \sum_{i,j} |O_{i,j}| \leq d^L \|O\|_F \leq d^{3L/2}$ holds from the Cauchy-Schwarz inequality, where $\|X\|_F = \sqrt{\text{Tr}[X^\dagger X]}$ is the Frobenius norm. It follows from Lems. 3 and 6 that $\nu_{d,L}^{*s}$ is a d^{-Lk} -approximate k -design. Therefore, for $1 \leq m \leq k/2$, we obtain

$$\begin{aligned} \Pr_{U \sim \nu_{d,L}^{*s}} [\langle \psi | U^\dagger O U | \psi \rangle \geq a] &\leq a^{-2m} \left\{ \left(\frac{m}{d^L} \right)^m + (d^L)^{3m-2k} \right\} \\ &\leq 2 \left(\frac{m}{d^L a^2} \right)^m. \end{aligned} \quad (\text{A13})$$

The inequality holds trivially for $m = 0$ if we define $0^0 = 1$. ■

Remark 9. The right-hand side of Eq. (A10) takes its minimal value $\simeq 2e^{-d^L a^2/e}$ at $m = m_0 \simeq d^L a^2/e$. Therefore, when $k \geq 2m_0$, the upper bound becomes double-exponentially suppressed with respect to L .

Appendix B: Covering number of ϵ -net for matrix product states

We consider a one-dimensional chain of L sites, each with a local dimension d . Let $A = (A_i^{\sigma_i})_{i,\sigma_i}$ be a tensor, where $A_i^{\sigma_i}$ is a $D_i \times D_{i+1}$ complex matrix with $D_i = \min\{d^{i-1}, d^{L-i+1}, \chi\}$. We define \mathcal{T}_χ as a set of such tensors and \mathcal{S}_χ as a set of $A \in \mathcal{T}_\chi$ in the following canonical form:

$$\mathcal{S}_\chi := \left\{ A \in \mathcal{T}_\chi \mid \forall i \in \{1, \dots, L\} \quad \sum_{\sigma=1}^d A_i^\sigma A_i^{\sigma\dagger} = I_{D_i} \right\}. \quad (\text{B1})$$

Let \mathcal{M}_χ be a set of normalized (OBC-)MPSs with a bond dimension less than or equal to χ . We define a map $|\psi_\bullet\rangle$ from a tensor to a state:

$$|\psi_\bullet\rangle : \mathcal{S}_\chi \rightarrow \mathcal{M}_\chi, \quad A \mapsto \sum_{\{\sigma_i\}} A_1^{\sigma_1} \cdots A_L^{\sigma_L} |\sigma_1 \cdots \sigma_L\rangle. \quad (\text{B2})$$

Note that an MPS in the canonical form is already normalized. The map $|\psi_\bullet\rangle$ is surjective since any quantum state $|\Psi\rangle \in \mathcal{M}_\chi$ can be represented in the canonical form [53].

For a tensor $A \in \mathcal{T}_\chi$, we define its norm as follows:

$$\|A\| := \sqrt{\sum_{i=1}^L \sum_{\sigma_i=1}^d \|A_i^{\sigma_i}\|_F^2}. \quad (\text{B3})$$

Then, any tensor $(A_i^\sigma)_{\sigma=1}^d$ in the canonical form satisfies the following property:

$$\sum_{\sigma=1}^d \|X A_i^\sigma\|_F^2 = \|X\|_F^2. \quad (\text{B4})$$

Substituting $X = I_{D_i}$ in Eq. (B4), we have

$$A \in \mathcal{S}_\chi \Rightarrow \|A\| \leq R_\chi := \sqrt{L\chi}. \quad (\text{B5})$$

Now, we show the following lemma.

Lemma 10. *The map $|\psi_\bullet\rangle$ is \sqrt{L} -Lipschitz, that is,*

$$\forall A, B \in \mathcal{S}_\chi, \quad \| |\psi_A\rangle - |\psi_B\rangle \| \leq \sqrt{L} \|A - B\|. \quad (\text{B6})$$

Proof. By employing the telescoping sum, we have

$$\begin{aligned} & \| |\psi_A\rangle - |\psi_B\rangle \| \\ &= \left\| \sum_{\{\sigma_i\}} (A_1^{\sigma_1} \cdots A_L^{\sigma_L} - B_1^{\sigma_1} \cdots B_L^{\sigma_L}) |\sigma_1 \cdots \sigma_L\rangle \right\| \\ &= \left\| \sum_{i=1}^L \sum_{\{\sigma_i\}} A_1^{\sigma_1} \cdots A_{i-1}^{\sigma_{i-1}} (A_i^{\sigma_i} - B_i^{\sigma_i}) B_{i+1}^{\sigma_{i+1}} \cdots B_L^{\sigma_L} |\sigma_1 \cdots \sigma_L\rangle \right\| \\ &\leq \sum_{i=1}^L \left\| \sum_{\{\sigma_i\}} A_1^{\sigma_1} \cdots A_{i-1}^{\sigma_{i-1}} (A_i^{\sigma_i} - B_i^{\sigma_i}) B_{i+1}^{\sigma_{i+1}} \cdots B_L^{\sigma_L} |\sigma_1 \cdots \sigma_L\rangle \right\|. \end{aligned} \quad (\text{B7})$$

Let us define

$$\Delta_i^{\sigma_i} := A_i^{\sigma_i} - B_i^{\sigma_i}, \quad (\text{B8})$$

$$|\delta_i \psi\rangle := \sum_{\{\sigma_i\}} A_1^{\sigma_1} \cdots A_{i-1}^{\sigma_{i-1}} \Delta_i^{\sigma_i} B_{i+1}^{\sigma_{i+1}} \cdots B_L^{\sigma_L} |\sigma_1 \cdots \sigma_L\rangle. \quad (\text{B9})$$

Then it suffices to evaluate $\sum_{i=1}^L \| |\delta_i \psi\rangle \|$. By repeatedly using Eq. (B4), we obtain

$$\begin{aligned} \| |\delta_i \psi\rangle \|^2 &= \sum_{\{\sigma_i\}} \| A_1^{\sigma_1} \cdots A_{i-1}^{\sigma_{i-1}} \Delta_i^{\sigma_i} B_{i+1}^{\sigma_{i+1}} \cdots B_L^{\sigma_L} \|^2_F \\ &= \sum_{\sigma_1, \dots, \sigma_i} \| A_1^{\sigma_1} \cdots A_{i-1}^{\sigma_{i-1}} \Delta_i^{\sigma_i} \|^2_F. \end{aligned} \quad (\text{B10})$$

Then, we define

$$P_i := \sum_{\sigma_1, \dots, \sigma_{i-1}} (A_1^{\sigma_1} \cdots A_{i-1}^{\sigma_{i-1}})^\dagger (A_1^{\sigma_1} \cdots A_{i-1}^{\sigma_{i-1}}). \quad (\text{B11})$$

By construction, P_i is positive semidefinite, and from Eq. (B4) we have $\text{Tr}[P_i] = 1$. Therefore, $O_{D_i} \preceq P_i \preceq I_{D_i}$ holds, where $X \preceq Y$ means that $Y - X$ is positive semidefinite. It follows that

$$\begin{aligned} \| |\delta_i \psi\rangle \|^2 &= \sum_{\sigma_i} \text{Tr} [\Delta_i^{\sigma_i \dagger} P_i \Delta_i^{\sigma_i}] \\ &\leq \sum_{\sigma_i} \text{Tr} [\Delta_i^{\sigma_i \dagger} \Delta_i^{\sigma_i}] \\ &= \sum_{\sigma_i} \|\Delta_i^{\sigma_i}\|_F^2. \end{aligned} \quad (\text{B12})$$

Finally, by using the Cauchy-Schwarz inequality, we obtain

$$\begin{aligned} \| |\psi_A\rangle - |\psi_B\rangle \| &\leq \sqrt{L} \sqrt{\sum_{i=1}^L \| |\delta_i \psi\rangle \|^2} \\ &\leq \sqrt{L} \sqrt{\sum_{i=1}^L \sum_{\sigma_i} \|\Delta_i^{\sigma_i}\|_F^2} \\ &= \sqrt{L} \|A - B\|. \end{aligned} \quad (\text{B13})$$

■

We fix $\epsilon \in (0, 2]$ and define $\mathcal{N}_{\chi, \epsilon}$ to be one of the maximal ϵ/\sqrt{L} -separated subsets of \mathcal{S}_χ , that is, for any $P, Q \in \mathcal{N}_{\chi, \epsilon}$ with $P \neq Q$, we have $\|P - Q\| > \epsilon/\sqrt{L}$. Now, for any $|\Psi\rangle \in \mathcal{M}_\chi$ there exists $A \in \mathcal{S}_\chi$ such that $|\psi_A\rangle = |\Psi\rangle$ due to the surjectivity of $|\psi_\bullet\rangle$. Then, there exists $A' \in \mathcal{N}_{\chi, \epsilon}$ such that $\|A - A'\| \leq \epsilon/\sqrt{L}$ because otherwise $\mathcal{N}_{\chi, \epsilon} \cup \{A\}$ would become a larger ϵ/\sqrt{L} -separated set of \mathcal{S}_χ . It follows from Lem. 10 that $\||\Psi\rangle - |\psi_{A'}\rangle\| = \||\psi_A\rangle - |\psi_{A'}\rangle\| \leq \epsilon$. Therefore, $|\psi_{\mathcal{N}_{\chi, \epsilon}}\rangle := \{|\psi_A\rangle \mid A \in \mathcal{N}_{\chi, \epsilon}\}$ is an ϵ -net of \mathcal{M}_χ .

A tensor $A = (A_i^{\sigma_i})_{i, \sigma_i} \in \mathcal{T}_\chi$ has $d \sum_{i=1}^L D_i D_{i+1}$ complex matrix elements. For each $A \in \mathcal{T}_\chi$, we define an $f_\chi := 2d \sum_{i=1}^L D_i D_{i+1}$ -dimensional real vector \mathbf{v}_A whose elements consist of the real and imaginary parts of the matrix elements of A . Let $B(\mathbf{v}, r)$ be an f_χ -dimensional ball of radius r which is centered at \mathbf{v} . Then, it follows from $\|\mathbf{v}_A\| = \|A\|$ and Eq. (B5) that

$$A \in \mathcal{S}_\chi \implies \mathbf{v}_A \in B(\mathbf{0}, R_\chi). \quad (\text{B14})$$

Since balls in the set $\{B(\mathbf{v}_A, \epsilon/2\sqrt{L}) \mid A \in \mathcal{N}_{\chi, \epsilon}\}$ are disjoint and contained in the ball $B(\mathbf{0}, R_\chi + \epsilon/2\sqrt{L})$, we have by a volume argument

$$|\mathcal{N}_{\chi, \epsilon}| \leq \frac{(R_\chi + \epsilon/2\sqrt{L})^{f_\chi}}{(\epsilon/2\sqrt{L})^{f_\chi}}. \quad (\text{B15})$$

It follows from $\||\psi_{\mathcal{N}_{\chi, \epsilon}}\rangle\| \leq |\mathcal{N}_{\chi, \epsilon}|$ and $f_\chi \leq 2dL\chi^2$ that

$$\||\psi_{\mathcal{N}_{\chi, \epsilon}}\rangle\| \leq \left(\frac{3L\sqrt{\chi}}{\epsilon}\right)^{2dL\chi^2}. \quad (\text{B16})$$

Appendix C: Derivation of Eq. (5)

We denote

$$P_{\chi, a} := \Pr_{U \sim \nu_{d, L}^{*s}} \sup_{|\psi\rangle \in \mathcal{M}_\chi} \left[\left| \langle \psi | U^\dagger O U | \psi \rangle - \frac{\text{Tr}[O]}{d^L} \right| \geq \Delta_O a \right] \quad (\text{C1})$$

as the probability of finding a burst that is larger than or equal to $\Delta_O a$ starting from one of the pure states in \mathcal{M}_χ . Using $|\langle \psi | O | \psi \rangle - \langle \psi' | O | \psi' \rangle| \leq \Delta_O \|\psi - \psi'\|$ and applying the union bound to Eqs. (A10) and (B16), we have

$$\begin{aligned} P_{\chi, a} &\leq \Pr_{U \sim \nu_{d, L}^{*s}} \left[\exists |\psi'\rangle \in |\psi_{\mathcal{N}_{\chi, \epsilon}}\rangle \text{ s.t. } \left| \langle \psi' | U^\dagger O U | \psi' \rangle - \frac{\text{Tr}[O]}{d^L} \right| \geq \Delta_O (a - \epsilon) \right] \\ &\leq \||\psi_{\mathcal{N}_{\chi, \epsilon}}\rangle\| \Pr_{U \sim \nu_{d, L}^{*s}} \left[\left| \langle \psi' | U^\dagger O U | \psi' \rangle - \frac{\text{Tr}[O]}{d^L} \right| \geq \Delta_O (a - \epsilon) \right] \\ &\leq 2 \left(\frac{3L\sqrt{\chi}}{\epsilon} \right)^{2dL\chi^2} \left\{ \frac{m}{d^L(a - \epsilon)^2} \right\}^m \end{aligned} \quad (\text{C2})$$

for all $0 < \epsilon < a$. By minimizing the right-hand side with respect to ϵ , we obtain

$$P_{\chi, a} \leq 2 \left(\frac{3}{d\chi^{3/2}} \right)^{2dL\chi^2} \left(\frac{1}{md^L} \right)^m \left(\frac{dL\chi^2 + m}{a} \right)^{2(dL\chi^2 + m)}. \quad (\text{C3})$$

Since d and χ do not depend on the system size, the logarithm of $P_{\chi, a}$ is approximately bounded as

$$\ln P_{\chi, a} \lesssim -m \ln(md^L) + 2(dL\chi^2 + m) \ln \frac{dL\chi^2 + m}{a}. \quad (\text{C4})$$

Equation (5) in the main text is thus proved.